

# Experimental Investigation of Partially CFRP Wrapped Steel HSS Braces for Seismic Performance Improvement



**C. Haydaroglu**

*Istanbul Technical University, Institute of Science and Technology, Istanbul, 34469, Turkey*

**O.C. Celik**

*Istanbul Technical University, Faculty of Architecture, Istanbul, 34437, Turkey*

## **SUMMARY:**

This study describes an experimental investigation into the seismic retrofit of locally slender tubular steel braces using advanced composites. Wrapping the critical sections of a tubular brace (both in the net and mid-span sections) with CFRP sheets are proposed for both delaying local buckling and potential net section failures at brace-to-gusset-connections. Three large-scale specimens were designed per AISC specification and subjected to quasi-static reversed cyclic testing protocol to compare their inelastic performances. All brace specimens, two partially retrofitted ones and the bare one, showed similar hysteretic behavior, revealing that large local slenderness significantly reduced the effectiveness of partial CFRP wraps. Partially external CFRP retrofit did not effectively worked at local slenderness value of 20. Overall ductility increased, but no significant increase in hysteretic energy dissipation was observed (max. 7%). Experimental fracture lives of the retrofitted specimens were higher (max. 7%) than that of the reference specimen.

*Keywords: Inelastic buckling, tubular braces, CFRP, retrofit, slenderness*

## **1. INTRODUCTION**

Braced frames are commonly used as lateral load carrying systems in steel structures mainly because of their high lateral strength and stiffness. These braces experience large axial cyclic displacements in tension and compression under earthquake excitations. Square HSS braces having equal sectional properties in major directions are obviously preferred in structural applications because of their good sectional properties, high strength, and high capacity/weight ratio. Previous experimental and theoretical studies have shown that hysteretic behavior of tubular braces is significantly affected by the global and local slenderness of the brace (Tremblay, 2002 and Celik et al., 2005, Haddad et al., 2011). Depending on their global and local slendernesses, tubular braces have unequal and complex hysteretic behavior in tension and in compression due to inelastic buckling. Critical sections in these members are brace-to-gusset connection and middle regions. Net section of the brace may govern the behavior especially under tension loading since a net section failure may prematurely occur. Moreover, a local buckling may occur especially in the middle section of non-compact sections (i.e. sections with large local slenderness ratios), and in the subsequent cycles, middle region of the brace section could fail due to repeated compression and tension effects during earthquakes. This behavior may lead to a lower fracture life, resulting in a possible soft story mechanism due to abrupt change in story strength and stiffness.

Using advanced composites, carbon fibre (CFRP) or glass fibre (GFRP), in retrofit of steel members is relatively newer than in retrofit of concrete and masonry members in the construction industry. Quite limited studies are available for CFRP applications in steel members including braces (El-Tawil et al., 2011, Harries et al., 2008, Shaat and Fam, 2009 and 2006, Teng and Hu, 2006). Especially CFRP members have obviously high tension capacity not only in sheet but also in laminate forms. To improve hysteretic behavior by both delaying local buckling and net section failures, critical sections of the braces (i.e. brace-to-gusset net sections and the mid-span area of the brace where local buckling

is expected), could be retrofitted with CFRP members. For this purpose, CFRP laminates serving as sectional reinforcement could be epoxy-bonded around the net sections and then wrapped with CFRP sheets to prevent or delay debonding. As for the mid-span section, a part of the mid-span region could be partially (say a percentage of the clear brace length) wrapped with CFRP sheets to delay local buckling, obtain longer fracture life, and higher cumulative energy dissipation.

An experimental program incorporating three large-scale, relatively stocky and locally slender, square HSS brace specimens having a section of 70mm x 70mm x 3mm and designed to AISC provisions is conducted to investigate the potential advantages of CFRP retrofit of steel tubular braces. The specimens were cyclically tested under quasi-static displacement histories per ATC-24 (1992). All tests were carried out in the Structural and Earthquake engineering Laboratory (STEEL) of Istanbul Technical University.

This paper reports on the cyclic inelastic behavior of partially CFRP retrofitted/wrapped square HSS braces. The obtained strength, stiffness, maximum displacement ductilities, cumulative dissipated energies, and fracture lives are compared. Experimental results show that, at the same ductility levels, the proposed CFRP retrofit scheme for HSS braces did not help much as the cumulative energy dissipation and fracture life of locally slender braces are almost the same (max 7% more only). This is attributed to large slenderness ratios (i.e. 20, as the case in this paper) since local strains get excessive values after severe local buckling and cannot be controlled by the CFRP members anymore. However, the retrofit of smaller slenderness ratio HSS braces using CFRP members is more effective.

## 2. EXPERIMENTAL PROGRAM

### 2.1. Specimens and Test Setup

Three specimens (namely TB-1, TB-2, and TB-3) made of Fe37 grade steel were designed and constructed using square HSS braces. Locally available, non-compact square HSS braces having a width of  $b=70\text{mm}$  and a wall thickness of  $t=3\text{mm}$  were selected in this work since the purpose was to investigate local buckling behavior rather than net section behavior. Generic specimen properties and their retrofitted regions are given in Table 2.1.

**Table 2.1.** Specimens

Specimen	Section	KL/r	b/t	Slotted end retrofit	Mid-span retrofit
TB-1	Square HSS 70x70x3	50	20	Bare	Bare
TB-2				1 layer CFRP laminate + 2 layers CFRP wraps	450mm length of CFRP wrap (17%L)
TB-3				1 layer CFRP laminate + 2 layers CFRP wraps	900mm length of CFRP wrap (34%L)

All specimens were designed in accordance with the AISC-LRFD (2005) and AISC-Seismic Provisions (2005) as appropriate. Note that this study preceded the publication of the current AISC Code. Slotted end connection detail with 20mm slot length was selected in brace-to-gusset connections.

Gas metal arc welding and grade SG2 filler rod were used for fillet welds used in brace-to-gusset connections. Ultimate tensile strength of SG2 is given as  $550\text{N/mm}^2$ . All brace surfaces were cleaned and prepared by grit blasting (grade SA2.5), prior to CFRP application. MBrace Laminate LM10/1.4 CFRP has a modulus of elasticity (E) of  $165000\text{N/mm}^2$ , a tensile strength of  $2500\text{N/mm}^2$  and a maximum elongation of 1.5%. MBrace Fiber C1-23 CFRP has an E modulus of  $240000\text{N/mm}^2$ , tensile strength of  $3800\text{N/mm}^2$ , and a maximum elongation of 1.55% (BASF YKS, 2009). In TB-2 and TB-3, CFRP sheets were bonded to the brace surface using MBrace epoxy components.

A safety factor of 2.0 was used for the design of epoxy bonding and CFRP member cross-sectional areas. HSS members with cold formed sections have continuous weld line on one of member edges.

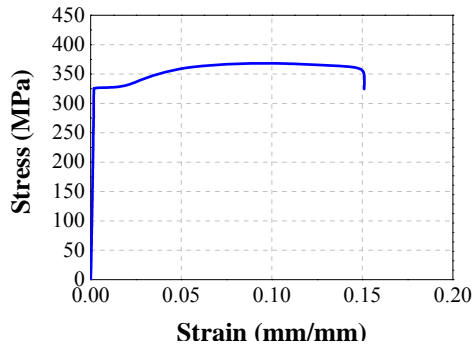


**Figure 1.** Average stress-strain curve and failure view of one coupon

Therefore, coupons were taken from two neighbouring edges not having weld line. ASTM A370-08a (2008) standard coupon tests provided average values of steel yield stresses of  $330\text{N/mm}^2$  (Fig. 1). The yield strength of the brace coupons was calculated using the 0.2% strain offset. As the yield value is larger than the design value for Fe37, all design checks were repeated prior to testing.

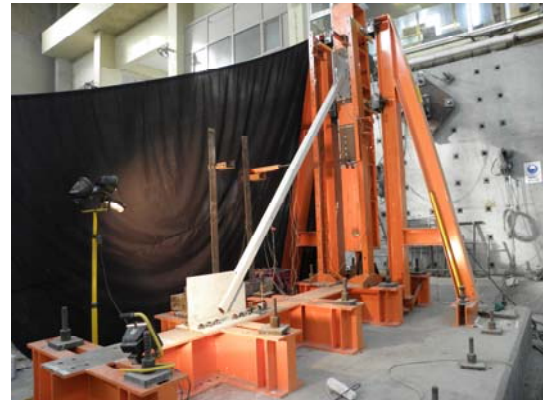
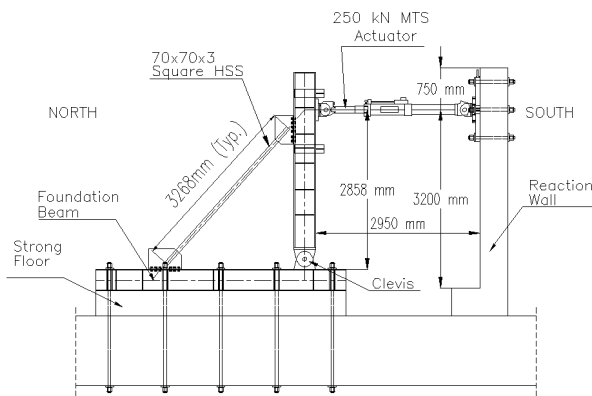


**Figure 2.** Test setup and overall view

For this experimental study, a special testing frame was designed and constructed in STEEL (Fig. 2). This frame was designed to accommodate different bracing sizes and lengths for future experiments.

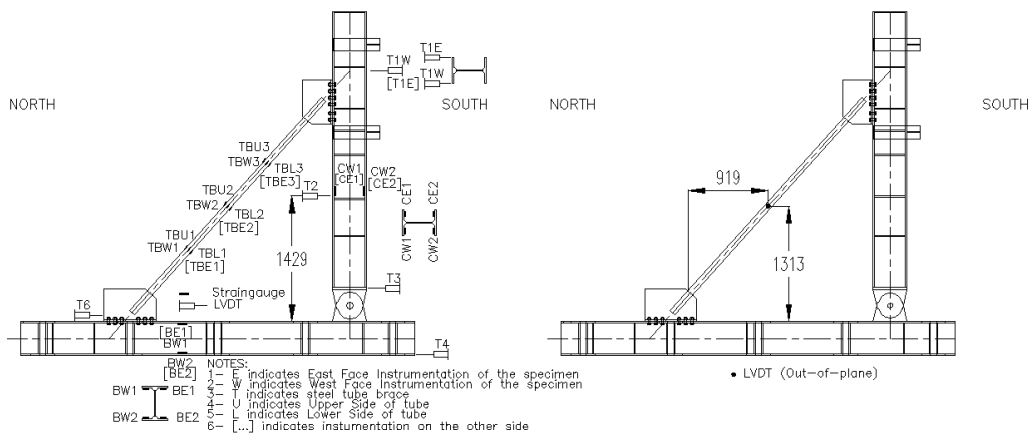


**Figure 3.** Instrumentation layout for the specimens

All members and connections were designed with a safety factor of at least 2.0. Loads were applied by a computer-controlled MTS hydraulic actuator, capable of producing up to 250kN. Instrumentation layout for all specimens is shown in Fig. 3.

## 2.2. Reversed Cyclic Testing

Each specimen was cyclically tested in accordance with the ATC-24 protocol. Top horizontal displacement is related to the brace axial displacement and was taken as the displacement control parameter. To facilitate comparison between the experimental results for all specimens the same cyclic displacement history that was applied to TB-1 was applied to TB-2 and TB-3. Loading protocol used for the specimens and the vertical lines showing failure displacement of each brace are depicted in Fig. 4. Material properties gained from the coupon tests were used in pushover analyses, performed to predict the yield displacement used to determine loading protocol of the specimens.

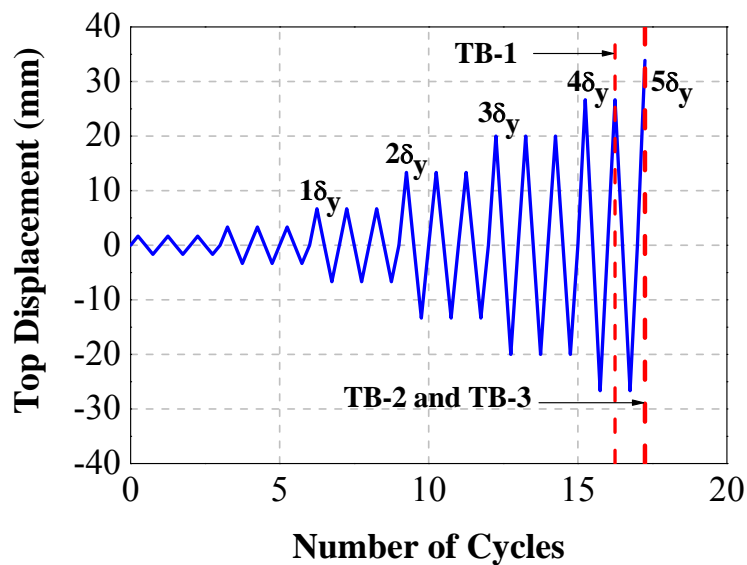


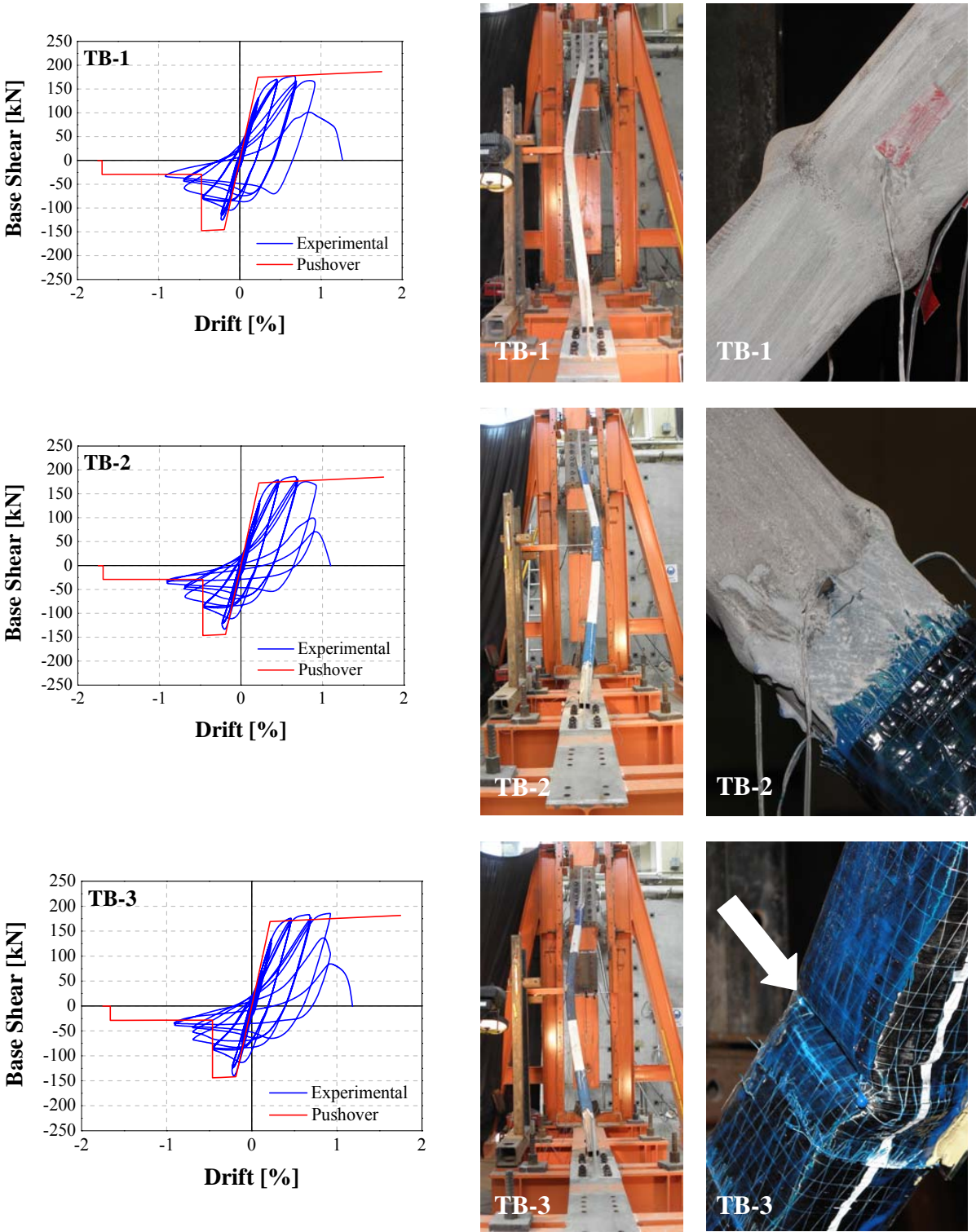
Figure 4. ATC-24 loading protocol for the specimens

## 2.1. Hysteretic Curves and Observations

For each specimen, experimental base shear versus lateral drift hysteresis, buckled shapes of the braces, and damage levels at fracture are shown in Fig. 5. Specimen TB-1 (the bare specimen) exhibited completely linear behavior until the yield (buckling) level. Note that, after buckling, the differences between tension and compression strengths were visible in the hystereses. The reached maximum tension and compression capacities are 178kN and 125kN, respectively. Occurrence of local buckling was observed at mid-span section at the first  $-3\delta_y$  displacement level, then inelastic strains rapidly accumulated in that region at subsequent loading cycles (Fig. 5c). In particular, due to the significant strain changes around the local buckling region, fracture initiation starting from the corners of local buckling side was observed at the last  $+3\delta_y$  displacement level. When the specimen reached to the peak target displacement value during the second cycle of  $+4\delta_y$ , a small portion of the section was standing in the mid-span region. Starting from here, TB-1 was subjected to tension load until it fractured. Finally, at displacement ductility of  $\mu=4$ , TB-1 fractured at mid-span local buckling region. During whole testing, no fracture initiation developed at the brace-to-gusset slotted end sections.

Specimen TB-2 (having a 450mm long CFRP sheet wrap at its mid-span region and CFRP plate+sheet reinforcement at brace-to-gusset connections) had no significant changes in hysteretic behavior in the elastic cycles. The maximum tension and compression capacities reached are 187kN and 135kN, respectively. The specimen experienced a global buckling prior to the occurrence of local buckling. A

local buckling plastic hinge developed outside the retrofitted region at  $-3\delta_y$  displacement level (Fig. 5c). As expected, the plastic hinge region shifted to a relatively less stiff region due to the existence of



a) Base shear vs. lateral drift hysteresis and FEMA pushover curves      b) Buckled shapes of braces at  $-3\delta_y$       c) Local buckling regions of braces

**Figure 5.** Hysteresis, FEMA pushover curves, buckled shapes, and local buckling regions of specimens



Although TB-3 (having a 900mm long CFRP sheet wrap at its mid-span region and CFRP plate+sheet reinforcement at brace-to-gusset connections) did not showed the most ductile behaviour due to its high local slenderness, TB-3 reached the maximum compression capacity (8% more). No significant change was observed in tension strength. Hysteretic behaviour was almost the same with TB-2. The reached maximum tension and compression capacities are 186kN and 141kN, respectively.

The specimen experienced local buckling at  $-3\delta_y$  displacement level at the middle section under the CFRP wrap (Fig. 5c). Fracture initiation was observed on the external confinement serving by CFRP wrap at  $-3\delta_y$  level and it fractured completely at  $-4\delta_y$  level. TB-3 fractured around the middle section at  $+5\delta_y$ .

Out-of-plane displacements of mid-span of the specimens could be of interest and were measured up to 150mm, the maximum capacity of the transducer. Fig. 6 shows out-of-plane displacements for each specimen considered here.

To compare hysteretic behaviors of the specimens around local buckling region, strain measurements that were recorded via strain gauges placed at the bulge side of mid-span are given in Fig. 6, too. Local buckling occurred at almost mid-span in TB-1 and TB-3 while local buckling shifted out of the CFRP wrap region in TB-2. In TB-2, mid-span strain gauge recorded almost linear behaviour, showing that CFRP wrapping effectively reduced the strains around the mid-span section and thus prevented the section from local buckling.

### 3. HYSTERETIC ENERGY DISSIPATION AND COMPARISON

Cumulative hysteretic energy dissipation values were calculated and given in Fig. 7 for comparison purposes. All specimens, TB-1, TB-2, and TB-3, dissipated almost similar amount of energies, this is because CFRP wraps on the mid-spans did not effectively delayed the occurrence of local buckling at large drifts due to large local slenderness of the sections. These three specimens were a small group of the experimental study of out of a total of 20 specimens (Haydaroglu et al. 2011a, 2011b and 2010). When all of the experimental results are evaluated and compared with each other, CFRP retrofit seems an effective way in order to delay or prevent local buckling at mid-span, and fracture at brace-to-gusset slotted end connection region in relatively small or moderate local slenderness ratios for HSS braces. However, the behaviors of the specimens tested here show that effectiveness of the CFRP confinement at mid-span is directly reduced by the large local slenderness of the tubular braces.

Furthermore, it seems that there is a local slenderness upper limit (say 20) that CFRP retrofit may not work much effectively as seen in this experimental work. CFRP retrofitting on TB-2 and TB-3, on the other hand, delayed the fracture until  $5\delta_y$  when compared to TB-1.

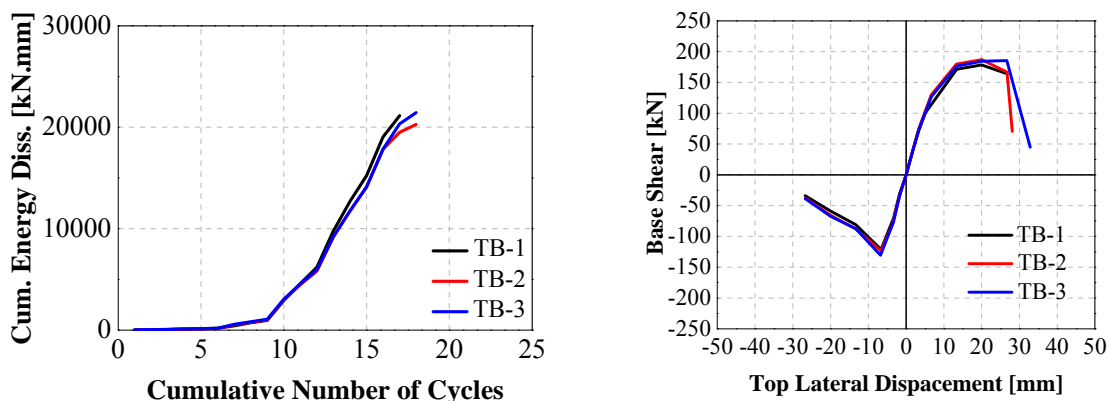


**Figure 7.** Cumulative energy dissipation and upper bound backbone curve for specimens

Degraded backbone upper bound curves are plotted and given in Fig. 7. As seen from that figure, no significant change in strength and stiffness are obtained which could be desirable in seismic retrofit applications since stiffness increases might result in larger earthquake forces in the system.

#### 4. EXPERIMENTAL FRACTURE LIFE AND EFFECTIVE LENGTH FACTORS

Experimental fracture lives ( $\Delta_f$ ) and effective buckling lengths of all specimens were calculated per the procedure given in Celik et al. (2005) and are shown in Table 4.1. Per this procedure, hysteresis curves are normalized by yield strength and the corresponding displacements are first constructed. The tension branch of the hysteresis is divided into two regions,  $\Delta_1$  and  $\Delta_2$ , defined at 1/3 of the yield strength. Here,  $\Delta_1$  is the tension deformation from the load reversal point to 1/3 of the yield strength point displacement, while  $\Delta_2$  is from 1/3 yield strength point to the unloading point. Then, experimental fracture life is calculated using

$$\Delta_f = \sum (0.1\Delta_1 + \Delta_2) \quad (4.1)$$

All specimens had almost equal fracture life (max. 7% more). External confinement of locally slender tubular braces (TB-2 and TB-3) did not effectively delay occurrence of local buckling and improve the fracture life, mainly because of the large local slenderness ratio of 20 that led to excessive local strains after severe local buckling and could not be controlled by the CFRP members anymore.

Experimental effective length factors are also possible from Table 4.1. These values have been obtained using the measured tube strain gauge data for the specimens. This was done by using axial strains below the yield level to calculate the bending moment diagram (i.e. elastic moments) on each brace. The maximum of the distances between two successive inflection points on the deflected shape was considered as the effective length of the brace as further discussed in Celik et al. (2005).

Since experimental effective length factor depends on several factors such as support conditions, testing possibilities etc., there exist some differences among the specimens. All K values are between 0.64 and 0.92 which could be expected from such an experimental work although it seems that the impact of CFRP wrapping has a negative effect on experimental effective length. This could be interpreted as an existence of possible support flexibility or possible rotations of gusset plates in the out of plane directions in TB-2 and TB-3 testing that increased the effective length factors.

**Table 4.1.** Experimental effective length factors and fracture lives

Specimen	Exp. Eff. Length Factor (K)	Normalized K	Experimental $\Delta_f$	Normalized $\Delta_f$
TB-1	0.642	0.696	26.92	1.002
TB-2	0.922	1	28.81	1.072
TB-3	0.904	0.980	26.87	1

#### 5. CONCLUSIONS

Inelastic behavior of partially CFRP retrofitted/wrapped square HSS braces is experimentally investigated. The obtained strength, stiffness, maximum displacement ductilities, cumulative dissipated energies, and fracture lives are compared. The following conclusions can be drawn from this study:

1. Although retrofitting HSS braces having relatively small or moderate local slenderness ratios using CFRP wraps shows promise in seismic rehabilitation applications, this experimental study

showed that proposed retrofitting technique did not effectively delay or prevent local buckling when tubular sections with large slenderness ratios are used (say 20 or larger).

2. Experimental results show that, at the same ductility levels, the proposed CFRP retrofit scheme for HSS braces did not help much as the cumulative energy dissipation and fracture life of locally slender braces are almost the same (max 7% more only).
3. CFRP retrofitting of tubular steel braces does not result in significant changes in the brace stiffness both in tension and compression that could be desirable in seismic retrofit applications.
4. CFRP wrapping in the transverse direction of the steel brace did not significantly affect the effective buckling length although some differences are obvious due to existing support conditions in the specimens.

## ACKNOWLEDGMENTS

This research was mainly supported by the Istanbul Technical University Research Fund. Tabosan, Borusan Mannesmann, BASF YKS, Cimtas, and As Civata provided the material used in the experiments. The authors thank the ITU-STEEL staff for their valuable help during testing. However, any opinions, findings, conclusions, and recommendations presented in this paper are those of the writers and do not necessarily reflect the views of the sponsors.

## REFERENCES

- AISC. (2005). ANSI/AISC 360-05 Specification for Structural Steel Buildings, American Institute of Steel Construction, Illinois, U.S.A.
- AISC. (2005). ANSI/AISC 341-05 Seismic Provisions for Structural Steel Buildings, American Institute of Steel Construction, Illinois, U.S.A.
- ASTM. (2008). A370-08a Standard Test Methods and Definitions for Mechanical Testing of Steel Products. American Society for Testing and Materials, PA, U.S.A.
- ATC. (1992). ATC-24 Guidelines for Cyclic Seismic Testing of Components of Steel Structures, Applied Technology Council, California, U.S.A.
- BASF YKS. (2009). Reinforcement Systems with Using Fibre Reinforced Polymers (FRP), Istanbul, Turkey.
- Celik, O.C., Berman, J.W. and Bruneau, M. (2005). Cyclic testing of braces laterally restrained by steel studs. *Journal of Structural Engineering* **131**, 1114-1124.
- El-Tawil, S., Ekiz, E., Goel, S. and Chao, S. (2011). Retraining local and global buckling behaviour of steel plastic hinges using CFRP. *Journal of Constructional Steel Research* **67**,261-269.
- Haddad, M., Brown, T. and Shrive, N. (2011). Experimental cyclic loading of concentric HSS braces. *Canadian Journal of Civil Engineering* **38**,110-123.
- Harries, K.A., Peck, A.J. and Abraham, E.J. (2008). Enhancing stability of structural steel sections using FRP. *Thin-Walled Structures* **47**,1092-1101.
- Haydaroglu, C., Turker, A., Taskin, K. and Celik, O.C. (2011a). Improving Hysteretic Behavior of Tubular Steel Braces Using Advanced Composites. *6th International Conference on Thin Walled Structures (ICTWS 2011)-Recent Research Advances and Trends. Vol II:* 691-698.
- Haydaroglu, C., Taskin, K. and Celik, O.C. (2011b). Ductility Enhancement of Round HSS Braces Using CFRP Sheet Wraps. *6th European Conference on Steel and Composite Structures (Eurosteel 2011). Vol B:* 1143-1148.
- Haydaroglu, C., Turker, A., Taskin, K. and Celik, O.C. (2010). Cyclic Testing of Tubular Steel Braces with CFRP Reinforced Net Sections. *4th International Conference on Steel & Composite Structures (ICSCS 2010)*. CD-ROM: SS-We010.
- Shaat, A. and Fam, A.Z. (2009). Slender steel columns strengthening using high-modulus CFRP plates for buckling controls. *Journal of Composites for Construction* **13**:1,2-12.
- Shaat, A. and Fam, A.Z. (2006). Axial loading test on short and long hollow structural steel columns retrofitted using carbon fibre reinforced polymers. *Canadian Journal of Civil Engineering* **33**:4,458-470.
- Teng, J.G. and Hu, Y.M. (2006). Behaviour of FRP-jacketed circular steel tubes and cylindrical shells under axial compression. *Construction and Building Materials* **21**,827-838.
- Tremblay, R. (2002). Inelastic seismic response of steel bracing members. *Journal of Constructional Research* **58**:5-8,665-701.